

See discussions, stats, and author profiles for this publication at: <https://www.researchgate.net/publication/304777824>

# Characterization of zeolites as environmental washcoat materials on cordierite ceramics.

Conference Paper · July 2016

CITATION

1

READS

183

8 authors, including:



**David Obada**

Ahmadu Bello University

98 PUBLICATIONS 1,460 CITATIONS

SEE PROFILE



**Mohammed Dauda**

Ahmadu Bello University

57 PUBLICATIONS 998 CITATIONS

SEE PROFILE



**Fatai Anafi**

Ahmadu Bello University

62 PUBLICATIONS 642 CITATIONS

SEE PROFILE



**Abdulkarim Salawu Ahmed**

Ahmadu Bello University

53 PUBLICATIONS 628 CITATIONS

SEE PROFILE

## **Characterization of zeolites as environmental washcoat materials on cordierite ceramics.**

*David O. Obada, Muhammad Dauda, Fatai O. Anafi and Samaila Umaru.*  
Department of Mechanical Engineering, Ahmadu Bello University, Zaria, Nigeria

*Abdulkarim S. Ahmed and Olusegun A. Ajayi*  
Department of Chemical Engineering, Ahmadu Bello University, Zaria, Nigeria.

*David Dodoo-Arhin*  
Department of Materials Science and Engineering, University of Ghana, Legon, Ghana.

*Abdulazeez Y. Atta*  
National Research Institute for Chemical Technology, Zaria, Nigeria.

### **ABSTRACT**

Small engines, such as conventional two stroke engines used in marine outboards and personal watercraft (PWC), are high polluters relative to their engine size and usage. Porous structures based on zeolites show promising characteristics as washcoat materials on cordierite ceramics for tail pipe exhaust emission control. This study reports the characterization of commercial grades of zeolites (Ammonium form of ZSM-5, Zeolite Y and Mordenite) and several transition phases of these zeolites aiming at their use as environmental washcoat materials. Thermogravimetry, X-ray diffraction, specific surface area and electron microscopy were used to characterize the zeolites. ZSM-5 shows high thermal and structural stability compared to the other zeolites investigated. As porogenic and increased active site agents, the transition phases showed a large quantity of meso-macro pores and a variation in the specific surface areas of the zeolites still large enough, which highlights their potential to be used in environmental catalysis.

**KEY WORDS:** Zeolite; transition phases; specific surface area; functional coating; porogenic; structural stability; thermal stability

### **INTRODUCTION**

Application of catalytic converters in two-stroke engines based on zeolite washcoat is becoming one of the most realistic methods of decreasing the levels of exhaust gas emissions. Zeolites are important in view of their industrial applications, such as in ion exchange, as molecular sieves, catalysts and adsorbents. Zeolites are unique crystalline compounds containing uniform sized micropores in their crystal structures. They show excellent cation exchange capacities, strong solid acidities, high adsorbing abilities and molecular sieving properties (Tominaga, 1993). Zeolite catalysts can be extruded or coated onto metal or ceramic substrates. The coating process involves preparation of zeolite slurry using a binder, usually colloidal silica or alumina, dipping the monolith, then drying and firing.

Various zeolites such as ZSM-5 (Seijger et al 2001; Garcí'a-Martí'nez

et al, 2001; Basaldella et al, 2002; Ulla et al, 2003; Ohman et al, 2004) and Mordenite (Ulla et al, 2004) have been successfully coated on supports by the in situ hydrothermal synthesis method. Moreover, in situ synthesized monolithic zeolite/support and modified zeolite/support have proven to be successful catalysts for many important reactions (van der Puil et al, 1996; Oudshoorn et al, 1999; Basaldella et al, 2002; Li et al, 2004; Li et al, 2005). Currently, the study of in situ synthesis focused on the optimized preparation of zeolite coatings (mainly ZSM-5) on various supports, such as honeycomb cordierite (Ulla et al, 2003; Ohman et al). Li et al, (2005) in their study explored a series of zeolites (Linde A, Linde Y, Mordenite and ZSM-5) which were synthesized on honeycomb cordierite supports by an in situ hydrothermal method in the absence of organic templates or zeolite seeds. They suggested that such a simple synthesis system would provide a better understanding of the growth of zeolites on supports.

Therefore the objective of this paper is to characterize commercial grade zeolites to predict which has more suitable properties for use as environmental materials. This is inspired by the development of ultra-stable type zeolites with much improved thermal and hydrothermal stability, and such zeolites show good potential for their use as washcoat materials.

### **MATERIALS AND METHODS**

Ammonium form of zeolites procured from Zeolyst Inc, USA was characterized by the thermo gravimetric /differential scanning calorimetry (TG/DSC), X-ray diffractometer (XRD), scanning electron microscopy (SEM) and BET- specific surface area analyzer. The as-received zeolites were first characterized by the TG/DSC (ramped from 200<sup>0</sup> C –1000<sup>0</sup> C) and XRD to ascertain their thermal and structural stability before been calcined at 600<sup>0</sup> C and 900<sup>0</sup> C. The thermal conditions chosen for the calcination of zeolite samples was guided by

the maximum temperature of exhaust gases from automotive tailpipes. Repeated XRD was carried out to determine whether the structures of the zeolites had been depleted by the application of heat. The samples were analyzed by X-ray diffraction. This was then followed by scanned images of the zeolites at different conditions. An investigation into the surface areas, pore sizes and pore volumes of these zeolites has also been explored.

Approximately 10mg of samples was used to perform thermogravimetric analysis (TGA) by the NETZSCH, STA 449 C Jupiter TG/DSC instrument at a heating rate of 10°C/min under an atmosphere of nitrogen. The samples have also been analyzed by X-ray diffractometry (Bruker AXS,D8 Advance) with CuK $\alpha$  radiation, 40kV and 30mA, time constant of 0.5s and crystal graphite monochromator to identify the phases present (metals and transition metal oxides). A step size of 0.02° 2 $\theta$  and a counting time of 4 seconds per step were applied over a 2 $\theta$  range of 5° to 90°.

The morphology of the zeolite samples have been evaluated by scanning electron microscopy (FEIXI-30).The zeolite samples were not coated prior to examination using the SEM as it was felt this could occlude some of the salient features, instead, a low acceleration voltage was used to avoid charging in the samples. This approach resulted in a good resolution of the zeolite features. For the SEM imaging for all zeolite samples, the samples were placed and set for vacuum pumping which took about 15mins This was systematically followed by adjusting parameters such as the focal length, contrast etc. which also was done for about 15mins.Then the observation and acquisition of images followed. The magnification for all zeolite samples tested was 10,000x.

Sample textural characteristics were determined by nitrogen gas adsorption (Autosorb - Quantachrome) at liquid nitrogen temperature. Nitrogen gas was used with a 22-point adsorption-desorption cycle. The samples were outgassed at 200 °C for 12 hours before each analysis. The zeolites' specific surface area, total pore volume and pore size and distribution was determined using a Micromeritics ASAP 2010 surface area analyzer. For the adsorption-desorption curves the adsorbate was N<sub>2</sub> and pore size distribution was calculated from the desorption branch using the Barret-Joyner-Halenda (BJH) model. Prior to the pore measurement, the samples were pre-treated by degassing at - 196 °C.

## RESULTS and DISCUSSION

### TG/DSC, XRD, SEM and BET of commercial grade of zeolites

**Thermo gravimetric analysis:** The feasibility of employing zeolites as promising washcoat materials was investigated in this section. As it can be seen from Figs. 1~2 depicting temperature profiles of the investigated ammonium forms of zeolites, there are no obvious weight loss in ZSM-5 and Zeolite Y samples. When the temperature reached 1000° C, the weight lost was just slightly less than 2%, so the DSC result also has no obvious change. The weight loss in these samples may have been caused by physically absorbed water or some organic impurities. However, the Mordenite sample presented in the temperature profile in Fig. 3 exhibited a 10% weight when the temperature reached 1000° C, so the DSC curve has a little rise between 500-900° C. This may be caused by some volatile materials burning off at this temperature. It is worthy of note that the thermal stability of these zeolite samples is due to the purity of the commercial grade zeolites which is devoid of organic impurities and physically absorbed water to a large extent.

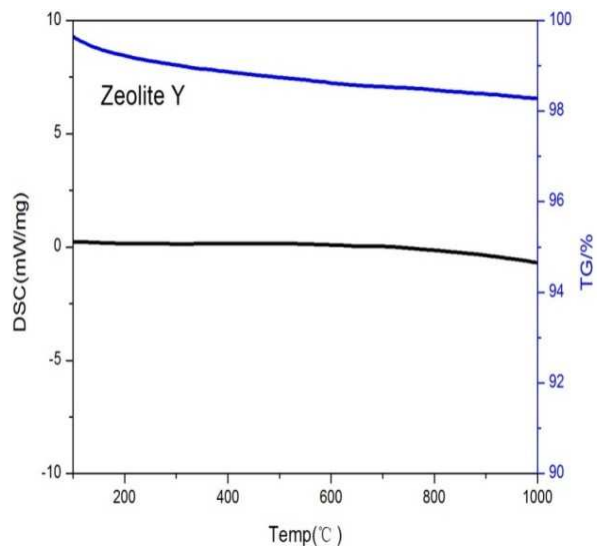


Fig. 1: TG/DSC curves of Zeolite Y

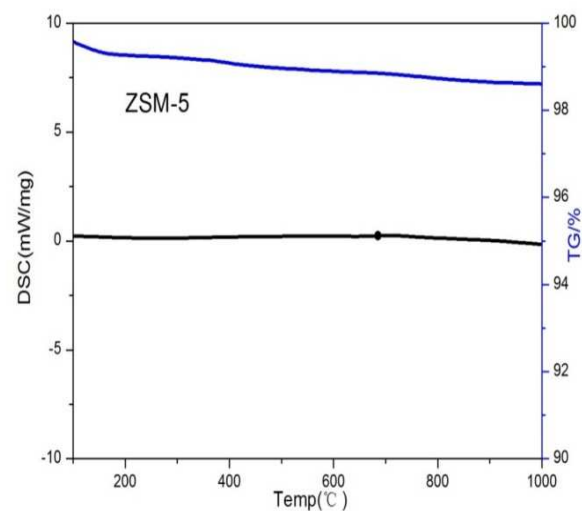


Fig. 2: TG/DSC curves of ZSM-5

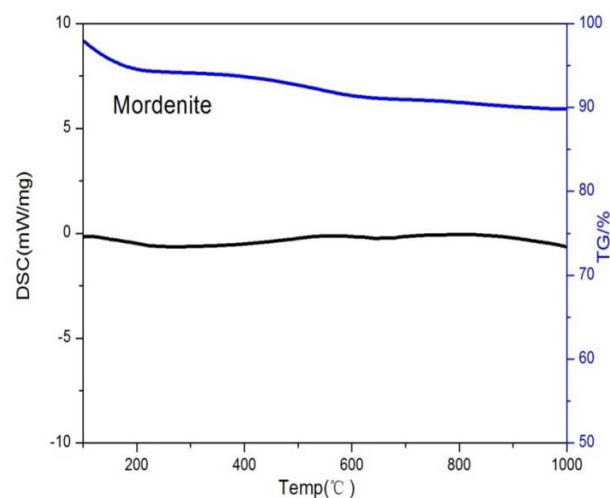


Fig. 3: TG/DSC curves of Mordenite.

**X-ray diffraction analysis:** The XRD patterns of the ammonium form of commercial zeolites ( $\text{NH}_4\text{-ZSM-5}(\text{SiO}_2/\text{Al}_2\text{O}_3=280)$ ,  $\text{NH}_4\text{-Mordenite}$  and  $\text{NH}_4\text{-Zeolite}(\text{SiO}_2/\text{Al}_2\text{O}_3=80)$ ) are as presented in Figs. 4~6. It should be noted that at calcination temperatures of  $600^\circ\text{C}$  and  $900^\circ\text{C}$ , the zeolites are converted to the hydrogen forms because for organic coating zeolites, the removal of the alkali metal cations normally takes place following the destruction of the organics by calcination. X-ray diffraction patterns (XRD) of the as-received zeolites show highly crystalline structure. ZSM-5 with characteristic peaks at  $7.88$ ,  $8.76$ ,  $23.04$ ,  $23.88$  and  $24.36^\circ$  (Wang *et al.*, 2000) can be seen at all conditions (as-received,  $600^\circ\text{C}$  and  $900^\circ\text{C}$ ). The intensity of peaks relatively at all conditions of treatment for ZSM-5 was not affected by the heat treatment. This is a strong statement of the structural and thermal stability of ZSM-5 under heating/calcination conditions.

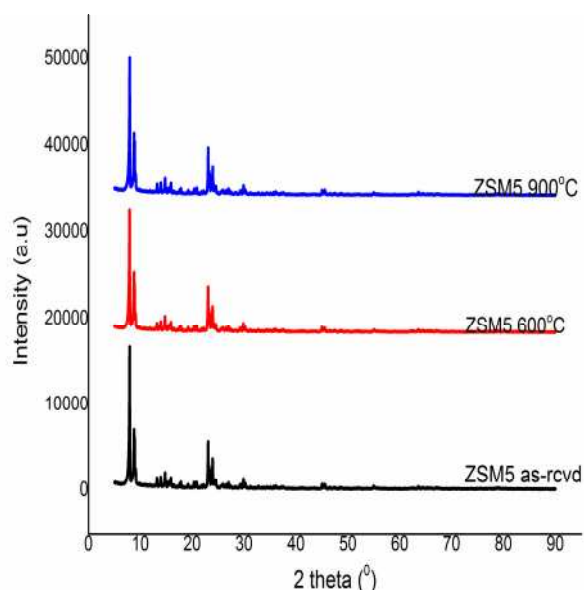


Fig. 4: XRD Patterns of ZSM-5(as received,  $600^\circ\text{C}$  and  $900^\circ\text{C}$ )

The Mordenite peaks found at Bragg's angle of about  $7$ ,  $10$ ,  $15$ ,  $22$ ,  $25$ ,  $26$ ,  $27$ ,  $32$ , and  $37^\circ$  (Corner *et al.*, 2014) (Fig.5) could be observed in the two of the three XRD patterns (as-received and  $600^\circ\text{C}$ ). However, the Mordenite peaks at sample calcined at  $900^\circ\text{C}$  showed depleted peaks at characteristic Bragg angles. The intensity of the characteristic peak of Mordenite at Bragg's angle of about  $7.0^\circ$  varied considerably among the samples. The sample calcined at  $900^\circ\text{C}$ , shows a significant increase in peak at  $7.0^\circ$  which may be due the increase in surface area of the zeolite, hence, some degree of increased crystallinity. XRD patterns of as-received samples and samples calcined at  $600^\circ\text{C}$  showed a similar trend with no significant disparity. However, the sample calcined at  $900^\circ\text{C}$  shows some minor depletion of other characteristic peaks implying a notable structural deterioration and instability of the zeolite at high temperatures.

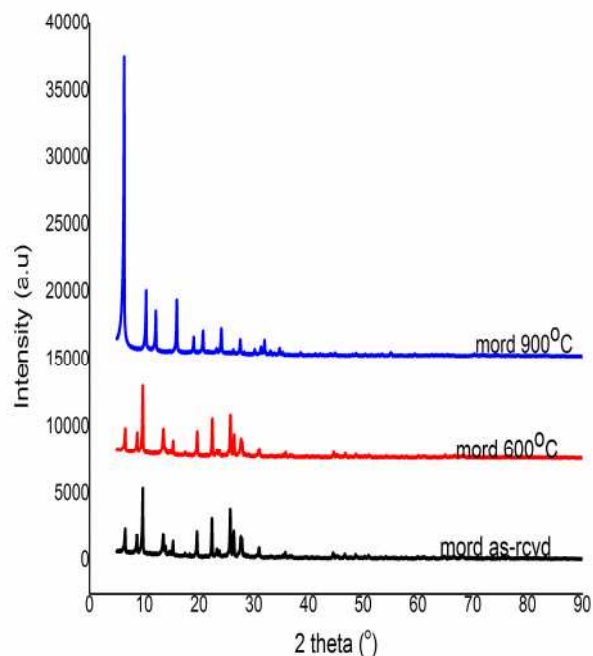


Fig. 5: XRD Patterns of Mordenite (as received,  $600^\circ\text{C}$  and  $900^\circ\text{C}$ )

Fig.6 shows zeolite Y peaks found at Bragg's angle of about  $6$ ,  $10$ ,  $12$ ,  $16$ ,  $19$ ,  $20$ ,  $24$ ,  $27$ ,  $31$  and  $32^\circ$  (Ginter *et al.*, 1992; Robson, 2001; Treacy and Higgins, 2001) could be observed in the three XRD patterns. However, the intensity of the characteristic peak of zeolite Y at Bragg's angle of  $6.13$  varied considerably among the samples. The sample calcined at  $900^\circ\text{C}$ , shows a significant reduction of characteristic peaks implying a notable structural deterioration and thermal instability of the zeolite at high temperatures. It is known that the XRD intensity of the characteristic peak of a mineral indicates the extent of crystallinity and the concentration of the crystalline content of the material.

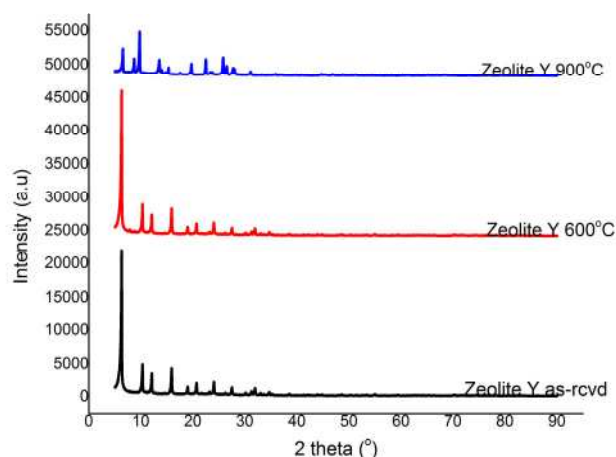


Fig. 6: XRD Patterns of ZeoliteY(as received,  $600^\circ\text{C}$  and  $900^\circ\text{C}$ )

**Scanning Electron Microscopy:** The SEM images of all zeolites tested at different conditions are as presented in Plate 1. ZM-as, ZM-600 and ZM-900 (NH<sub>4</sub> and H- ZSM-5), MD-as, MD-600 and MD-900 (NH<sub>4</sub> and H -Mordenite), ZY-as, ZY-600 and ZY-900 (NH<sub>4</sub> and H -ZeoliteY) represents as-received zeolite samples, zeolite samples calcined at 600 °C and zeolite samples calcined at 900 °C respectively. Comparatively, the SEM images of ZM-as, ZM-600 and ZM-900, show spherical morphology of the structures. The ZSM-5 zeolite at the points of imaging was thermally stable and the XRD patterns suggest the same. This reflects on the SEM images at different conditions. The sphere-like structure of the ZSM-5 zeolites at varying conditions remains relatively unaltered, which corroborates the thermal stability of the ZSM-5 samples at various temperature conditions.

Comparatively, the SEM images of MD-as, MD-600 and MD-900, show needle like morphology of the structures. The MD shows similar morphology for as-received samples and samples calcined at 600 °C except that the boundaries of the individual crystals were not as clearly obvious as in the micrograph of MD- 600. This is due to the relative

similarity in trend observed by the XRD pattern. The morphology of MD- 900 implies loss of crystallinity after calcinations. This further confirms the observation made in the analysis of the XRD of these samples that after calcinations at 900 °C a reduction in crystallinity was observed.

The SEM images of ZY-as shows clear picture of evenly distributed individual particles having regular tetrahedral shapes Therefore, it could be deduced from the images that the as-received (ZY-as) sample has an agglomerated tetrahedral morphology (Salaudeen, 2015). The image at ZY-600 shows a similar morphology of agglomerated particles with tetrahedral morphology. The morphology of sample ZY-900 also showed similar morphology except that the boundaries of the individual crystals were not as clearly obvious as in the micrograph of ZY-as and ZY-600. This implies loss of crystallinity after calcining at 900<sup>0</sup> C. This further confirms the observation made in the analysis of the XRD of these samples that after calcinations, a reduction in crystallinity was observed.

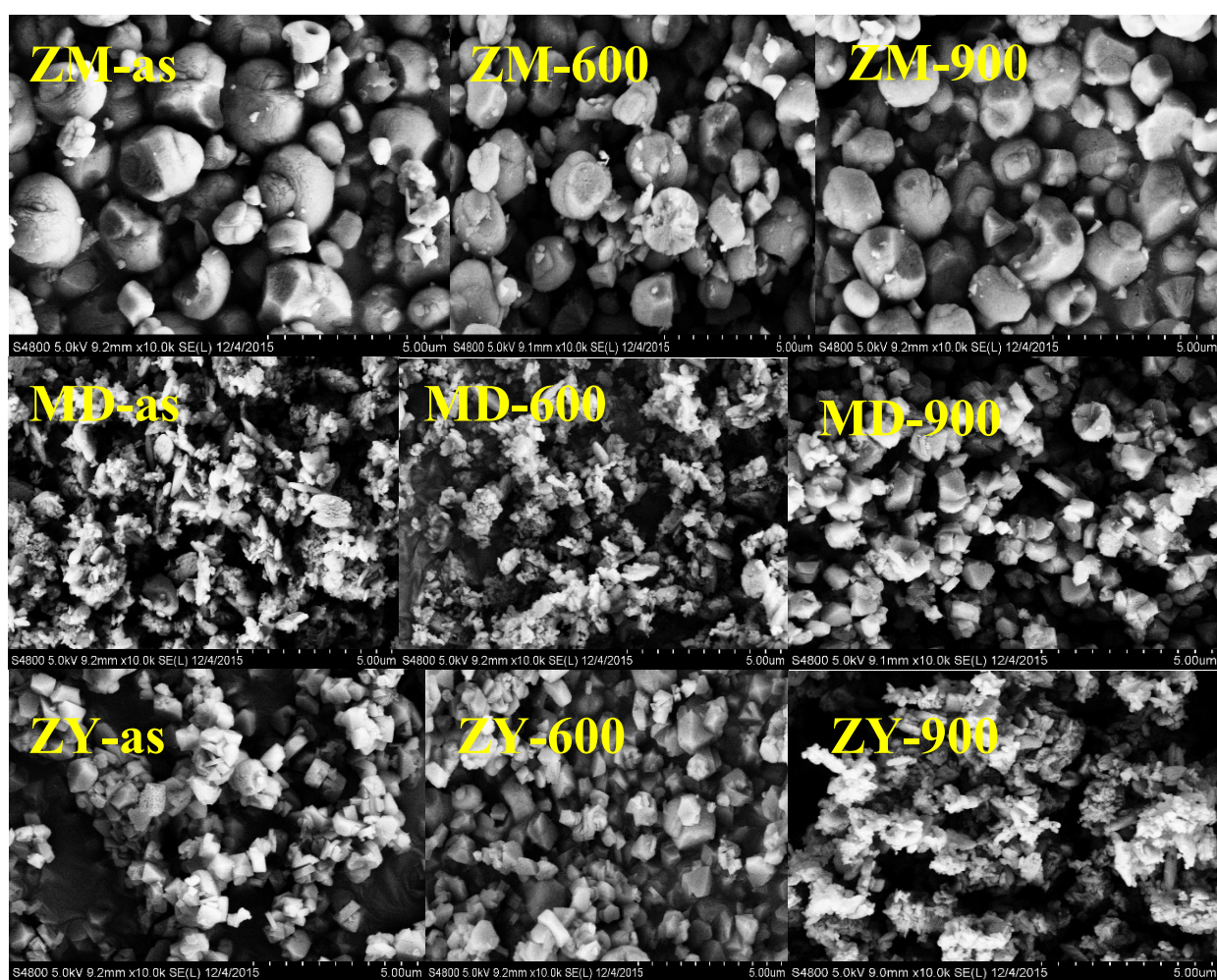


Plate 1: SEM images of ZSM-5, Mordenite and Zeolite Y (as received, 600 °C and 900 °C) at 10,000x; ZM-as, MD-as, ZY-as (as-received Zeolites), ZM-600, MD-600 and ZY-600 (zeolites calcined at 600 °C), ZM-900, MD-900 and ZY-900 (zeolites calcined at 900 °C).

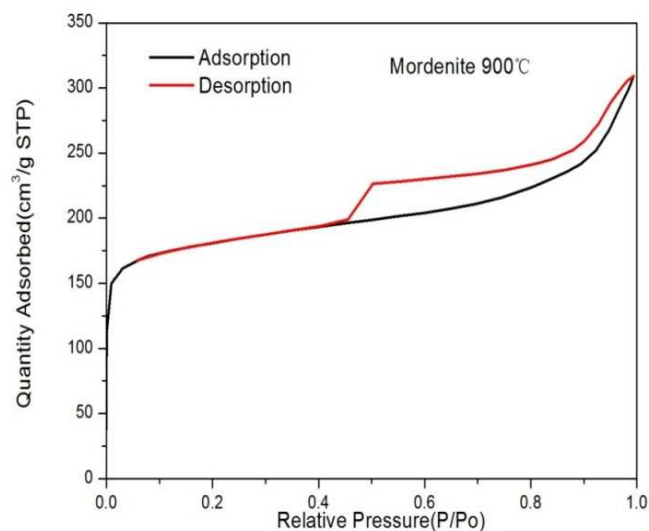
Table 1: Physicochemical properties of samples

Sample	BET Surface Area (m <sup>2</sup> /g)	Micropore area (m <sup>2</sup> /g)	Mesopore area (m <sup>2</sup> /g)	Micropore Volume (cm <sup>3</sup> /g)	Mesopore Volume (cm <sup>3</sup> /g)
ZM- as	418.5895	160.644	55.6863	0.110221	0.059334
ZM- 600 <sup>0</sup> C	362.0465	150.304	60.8960	0.115839	0.063054
ZM-900 <sup>0</sup> C	354.4291	141.816	194.9792	0.115852	0.127370
ZY- as	613.3555	120.905	166.8034	0.239108	0.256611
ZY- 600 <sup>0</sup> C	573.0639	120.786	175.1513	0.247085	0.271552
ZY-900 <sup>0</sup> C	417.8887	43.248	50.9796	0.092901	0.095549
MD- as	358.5678	28.435	32.3730	0.076085	0.077048
MD- 600 <sup>0</sup> C	438.3214	38.714	43.2349	0.089267	0.089717
MD-900 <sup>0</sup> C	614.0414	127.793	170.1379	0.249609	0.265601

**BET specific surface area:** Specific surface area of the zeolites was computed according to the BET method from the nitrogen adsorption isotherms obtained at 77 K, taking a value of 0.162 nm<sup>2</sup> for the cross-section of the adsorbed N<sub>2</sub> molecule at that temperature. Physicochemical properties of the various samples are summarized in Table 1. The BET surface area, microporous area and microporous volume of calcined zeolite samples (ZSM-5 and Zeolite Y) significantly decreased compared to the as-received form of these zeolite. The loss of BET surface areas, which was re-measured at different time intervals (600<sup>0</sup> C and 900<sup>0</sup> C) during the test, indicates the degree of thermal deterioration of the tested material. Also, the BET surface area, microporous area and microporous volume of calcined Mordenite increased compared to the as-received form of Mordenite. This can be as a result of the texture of micro pores of zeolite structure. As can be observed from table 1, BET surface area and micropore area of the ZM-as, ZM-600 and ZM-900 decreased progressively under the heat conditions while mesoporous area, micropore volume and mesoporous volume increased progressively. This observation is the inverse for Mordenite because ZSM-5 has the MFI (Mordenite Framework Inverted) structure. Also, BET surface area, micropore area and mesopore area of ZY-as, ZY-600 and ZY-900 decreased progressively under the heat conditions while micropore volume and mesoporous volume increased progressively. For Mordenite samples under the heat conditions, BET surface area, micropore area, mesopore area, micropore volume and mesopore volume all increased progressively (inverse of the ZSM-5 zeolite). These results suggest that the zeolites (ZSM-5, Zeolite Y and Mordenite) samples still showed relative thermal stability in terms of the loss of BET surface areas as it is noted that the degree of thermal deterioration caused a reduction in BET surface areas of the zeolites still sufficient enough to serve as washcoat materials on catalyst supports for enhanced active sites.

**Porosity Texture:** The porous structure of all samples was determined by N<sub>2</sub> adsorption-desorption measurements and the nitrogen isotherm for the samples is illustrated in Figs. 7–9. For the purpose of this study, N<sub>2</sub> adsorption-desorption measurements of samples at extreme calcination temperature is presented. According to IUPAC (Sing, 1985), the shape of the adsorption isotherm can be classified into one of six groups. Of these, the most common are type I (Langmuir) isotherms for purely microporous solids, and type IV for mesoporous solids in which capillary condensation takes place at higher pressures of adsorbate as well as a hysteresis loop. As is shown in Figs. 7–9, the adsorption volume at very low relative pressures ( $p/p_0 < 0.1$ ) is high, indicating the presence of microporous adsorption. Increasing the relative pressure causes capillary condensation, which illustrates type

IV behavior. All the zeolite samples show hysteresis loops that resembles the H4 type in the IUPAC classification. This can be attributed to the crystalline agglomerates that results in the mesoporous structure formed by the interparticle space and heat treatment that causes the formation of secondary pores. A distinct increase in the adsorbate volume in the low  $p/p_0$  region and the hysteresis loop in the high  $p/p_0$  region indicates the presence of micropores associated with mesopores. Therefore, the isothermal type of all samples is a combination of type I and type IV. The isotherm of all the samples shows a steep increase in N<sub>2</sub> adsorption at low relative pressure  $P/P_0$  between 0.0 and 0.4 exhibiting type I isotherm which is normally observed for microporous materials. However, the micropores in the samples are assumed not to be accessible to N<sub>2</sub> molecules at the analysis temperature, thus type I isotherm suggests the presence of small mesopores with size close to micropore range. At high relative pressure, in the range between 0.4 and 0.99, N<sub>2</sub> adsorption increases significantly displaying type IV isotherm with H<sub>3</sub> hysteresis due to capillary condensation of N<sub>2</sub> gas within the mesopores (Kruk and Jaroniec, 2001; Huang *et al.*, 2011). The absence of the plateau at  $P/P_0$  close to 1.0 suggests that the substrate particle consists of aggregated crystallites, this is also in agreement with Huang *et al.*, (2011)

Fig. 7: N<sub>2</sub> adsorption-desorption isotherms of Mordenite

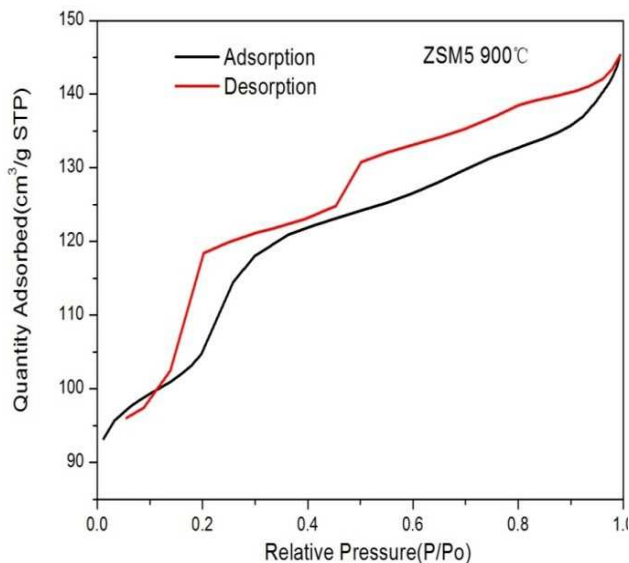


Fig. 8: N<sub>2</sub> adsorption-desorption isotherms of ZSM-5

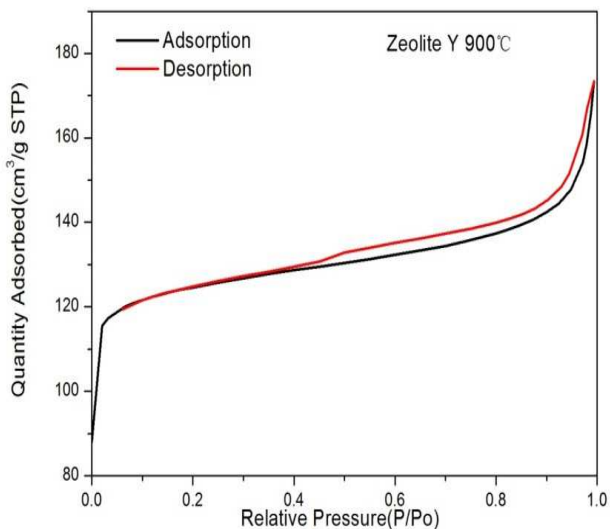


Fig. 9: N<sub>2</sub> adsorption-desorption isotherms of Zeolite Y

## CONCLUSIONS

The thermal stability of these zeolite samples as characterized by thermo gravimetry is due to the purity of the commercial grade zeolites which is devoid of organic impurities and to a large extent physically absorbed water. The intensity of peaks relatively at all conditions of treatment for ZSM-5 is not affected by the heat treatment. This is a strong statement of the structural stability of ZSM-5 under heat conditions. XRD patterns of Zeolite Y and Mordenite samples calcined at 600°C and 900°C showed depletion of characteristic peaks implying

a notable structural deformation and thermal instability of these zeolites at high temperatures. The sphere-like structure of the ZSM-5 zeolites at varying conditions remains relatively unaltered, which corroborates the thermal stability of the ZSM-5 samples at various temperature conditions. The morphology of sample ZY-900 also showed similar morphology except that the boundaries of the individual crystals were not as clearly obvious as in the micrograph of as received zeolite Y. The morphology of MD-900 implies loss of crystallinity after calcinations. The BET surface area, microporous area and microporous volume of calcined zeolite samples (ZSM-5 and Zeolite Y) significantly decreased compared to the as-received form of these zeolite. The loss of BET surface areas, which is re-measured at different time intervals (600°C and 900°C) during the test, indicates the degree of thermal deterioration of the tested material. Also, the BET surface area, microporous area and microporous volume of calcined Mordenite increased compared to the as-received form of Mordenite. This can be as a result of the texture of micro pores of zeolite structure. These results suggest that the ZSM-5 samples still showed relative thermal stability as shown by TG and XRD results and obviously in terms of the loss of BET surface areas as it is noted that the degree of thermal deterioration only caused a slight reduction of BET surface areas.

## REFERENCES

- Basaldella, E.I., Kikot, A., Quincoces, C.E., & Gonzalez, M. G. (2001) "Preparation of supported Cu/ZSM-5 zeolite films for DeNO<sub>x</sub> reaction". *SI* (4), 289-294.
- Basaldella, E.I.; Kikot, A.; Bengoa, J.F.; Tara, J.C. (2002). "ZSM-5 zeolite films on cordierite modules. Effect of dilution on the synthesis medium". *Mater. Lett.* 2002, 52, 350-354
- García-Martínez, J. Cazorla-Amoró, S.D. Linares-Solano, A. Lin, Y.S. *Micropor. Mesopor. Mater.* 42 (2001) 255.
- Ginter, D. M., Bell, A. T. and Radke, C. J. (1992), "Synthesis of Microporous Materials, Molecular Sieves". New York, Van Nostrand Reinhold
- Huang, C.H., Chang K., Ou H., Chiang Y., and Wang, C. (2011). "Adsorption of cationic dyes onto the mesoporous silica", *Microporous Mesoporous Mater.*, Vol. 141, p. 102-109.
- Kabwadza-Corner, P., Munthali, M.W., Johan, E. and Matsue, N. (2014) "Comparative Study of Copper Adsorptivity and Selectivity toward Zeolites". *American Journal of Analytical Chemistry*, 5, 95-405. <http://dx.doi.org/10.4236/ajac.2014.57048>
- Kruk, M. and Jaroniec, M. (2001). "Gas adsorption characterization of ordered organic-inorganic nano composite materials". *Chem. Mater.*, Vol. 13, p. 3169-3183.
- Lachman, I.M. Williams, J.L.(1992). "Extruded monolithic catalyst supports". *Catal. Today* 14, 317-329.
- Li, L., Chen, J., Zhang, S., Guan, N., Richter, M., Eckelt, R. and Fricke, R. (2004). "Study on metal-MFI/cordierite as promising catalysts for selective catalytic". *J. Catal.* 228 (2004) 12.
- Li L. J. Chen, S. Zhang, N. Guan, T. Wang, S. Liu (2004) "Selective Catalytic Reduction of Nitrogen Oxides from Exhaust of Lean Burn Engine over In-situ Synthesized Monolithic Cu-TS-1/cordierite", *Catal. Today* 90 207-213
- Li L.J. Chen, S. Xue B., Chen J.N. Guan, S. Zhang, Dexin L., and Feng H., (2005). "Direct synthesis of Zeolite Coatings on Cordierite Support by in-situ Hydrothermal Method". *Applied Catalysis A: General* 292 312-321
- Ohrman, O. Hedlund, J. Sterte, J. (2004) "Synthesis and evaluation of ZSM-5 films on cordierite monoliths", *Applied Catalysis A:*

- General, 270, 193-199.
- Oudshoorn, O.L.; Janissen, M.; Kooten, W.E.J.; Jansen, J.C.; van Bekkum, H.; van den Bleek, C.M.; Calis, H.P.A.. Source: *Chemical Engineering Science*, Volume 54, Number 10, 1 May 1999, pp. 1413-1418(6). Publisher: Elsevier
- Robson, H. (2001), "Verified Synthesis of Zeolitic Materials" 2nd edition. Published on behalf of the Synthesis Commission of the International Zeolite Association, Amsterdam, Netherlands, Elsevier.
- Salahudeen, N. (2015). "Development of Zeolite Y and ZSM-5 composite catalyst from Kankara Kaolin". A Ph.D thesis submitted to the Department of Chemical Engineering, Faculty of Engineering, Ahmadu Bello University, Zaria, Nigeria.
- Seijger, GBF., Oudshoorn, O.L., Boekhorst, A., Bekkum, H., Bleek, C.M., Calis, H.P.A. (2001). "Selective catalytic reduction of NO<sub>x</sub> over zeolite-coated structured catalyst packings". *Chemical Engineering Science*; 56: 849-57.
- Tominaga H. (Eds.) (1993), *Science and Applications of Zeolites*, Kodansha Scientific, Tokyo,
- Treacy, M. M. J. and Higgins, J. B. (2001), "Collection of Simulated XRD Powders for Zeolites". Published on behalf of the Synthesis Commission of the International Zeolite Association, Amsterdam, Netherlands, Elsevier.
- Ulla, MA. Miro', E. Mallada, R. Coronas, J. Santamaría, J.(2004) "Synthesis and characterization of ZSM-5 coatings onto cordierite honeycomb supports" *Applied Catalysis A: General* 253 (1), 257-269 Chem. Commun. 528.
- van der Puil, N. Creighton, E.J. . Sie, S.T Rodenburg, E.C. van Bekkum, H. Jansen, J.C (1996). *Chemical Engineering Science J. Chem. Soc., Faraday Trans.* 59, 2647-2657
- Wang, A., Liang D., Sun X., Zhang, T. (2000). "A new route for synthesis of ZSM-5 on cordierite honeycombs", *Chinese Journal of Catalysis*, 21 (5), 395-396.